JOURNAL OF MATERIALS SCIENCE 18 (1983) 1794–1802

Calculation of the forming limit curve at fracture

J. M. JALINIER
Laboratoire de Génie Physique et Mécaniques des Matériaux, GRECO CNRS "Grandes Déformations et Endommagement", Institut National Polytechnique de Grenoble (ENSIEG), 38402 Saint-Martin-d'Heres, France

The prediction of the forming limit diagram at fracture (FLDF) is of great importance, specially in cases where forming is controlled by fracture instead of necking. A physical model of coalescence is proposed in two cases of internal damage: (i) damage by decohesion of the particle matrix interface, and (ii) damage by failure of the particle. An analytical equation of the fracture curve is obtained in the case of damage by decohesion and this predicts a linear shape for the FLDF, which is in agreement with experiment. In contrast, in the case of damage by failure, a curved shape for the FLDF is obtained, which is also in agreement with experiment. Comparison of the models presented with other criteria is made.

1. Introduction

The deformation behaviour of a sheet metal can be represented in the diagram of the principal strains, ϵ_1 and ϵ_2, in the plane of the sheet. In this diagram (Fig. 1), two stages appear in a deformation process. The first stage, schematically represented in Fig. 1, is the quasi-uniform straining up to the occurrence of a neck as a result of a localized instability process. The points where the neck occurs for different linear strain paths is the forming limit diagram at necking (FLDN). Then, in the neck, because of the instability process, the strain path turn towards plane strain up to fracture. The level of the forming limit diagram at fracture (FLDF) cannot be directly determined by measurement of the strain ϵ_1 because of the presence of a severe strain gradient. A way to obtain the local strain ϵ_1 [1] is to measure the strain ϵ_2, which is roughly unchanged from necking to fracture and is without a severe strain gradient, and the local thickness strain ϵ_3. The strain ϵ_1 is then derived assuming constant volume, i.e. $\epsilon_1 + \epsilon_2 + \epsilon_3 = 0$.

Fig. 2 shows different FLDFs obtained experimentally. The shape can be linear or curved and in some cases (Fig. 2c) [2], the fracture curve cuts the necking curve, and in this event forming is limited by fracture before the required conditions for necking are achieved. In these cases it is particularly important to be able to predict the occurrence of fracture.

The fracture surface of the material always exhibits a ductile fracture process for the usual forming materials. The study of the FLDF is therefore a study of ductile fracture under a biaxial state of stress, taking into account the change in the strain path before and after necking. It requires the use of fracture criteria that can be divided into two main categories:

1. Macroscopic criteria based on a relationship between macroscopic variables at fracture (i.e energy, stress, strain, mechanical parameter of damage [3, 4]).

2. Microscopic criteria based on physical models of the coalescence of voids leading to ductile fracture.

The purpose of this paper is to use a physical model of void growth previously obtained [5] to establish a microscopic calculation of the FLDF. Comparison will be made with the calculations using macroscopic criteria and similarities between the two approaches will be shown.

2. Macroscopic criteria

Two main criteria will be used in this section:

0022–2461/83 $03.00 + .12

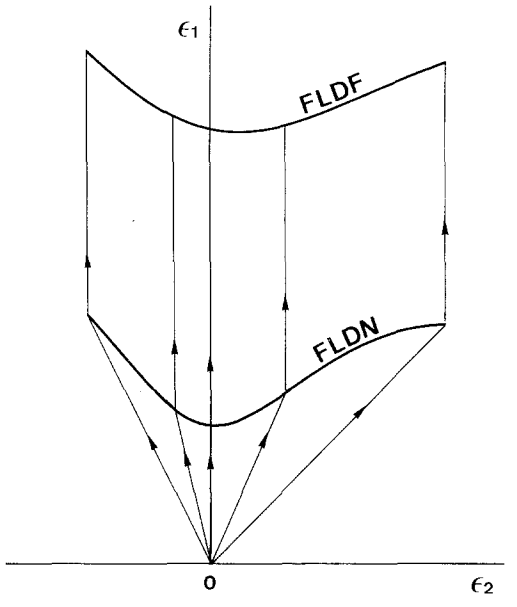

Figure 1 Schematic representation of the strain path followed before and after necking.

the Latham and Cockroft criterion [6], which is widely used, and the more recent Oyane criterion [7, 8]. Other criteria can also be used [9–11] in the biaxial state of stress but their predictions are too optimistic compared with experiment.

2.1. Latham and Cockroft criterion

The criterion is given by

$$\int_0^{\epsilon_{ef}} \sigma_e \left(\frac{\sigma_1}{\sigma_e}\right) d\epsilon_e = P \qquad (1)$$

where ϵ_{ef} is the equivalent strain at fracture, σ_1 the maximum principal stress, and P a constant

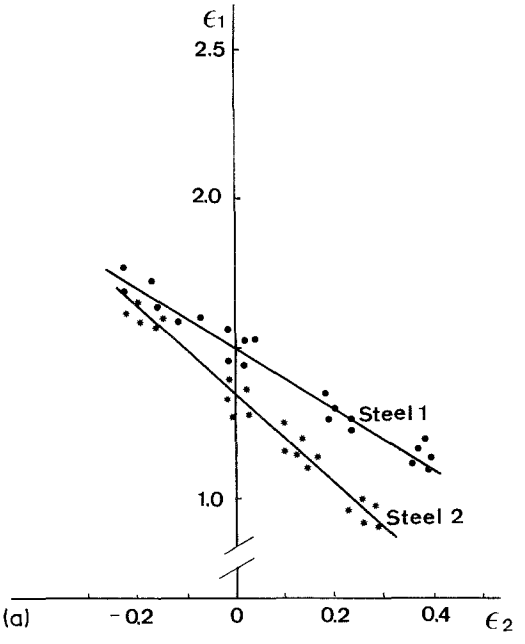

Figure 2 FLDF in the case of: (a) mild steels [1], (b) 3003 aluminium alloy, and (c) 5154-0 aluminium [2].

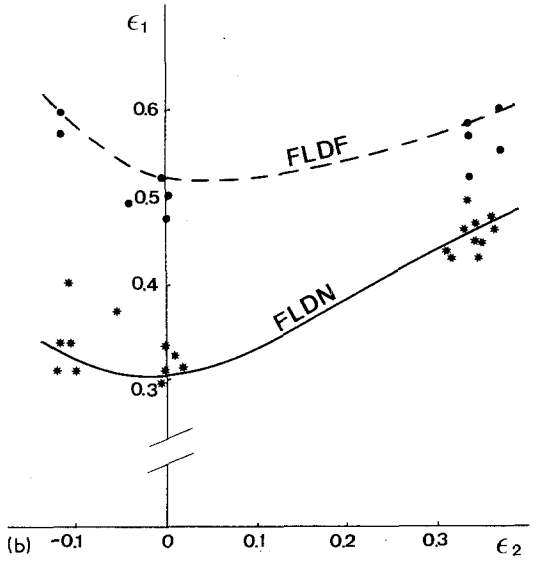

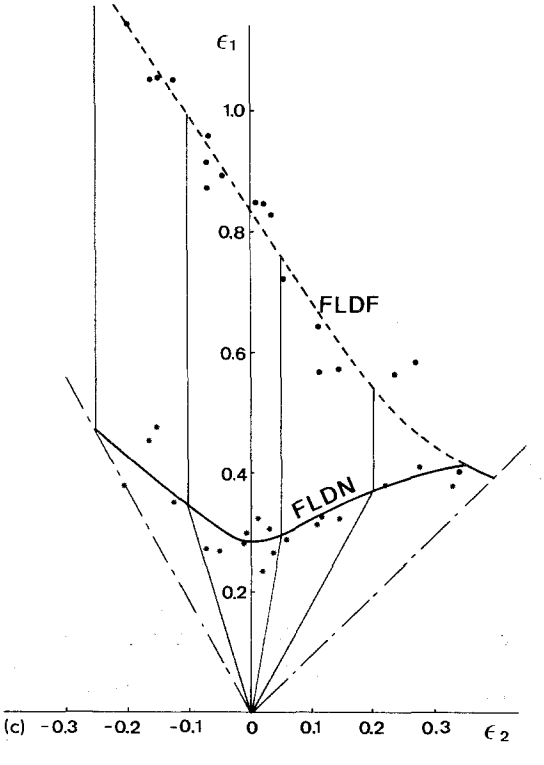

of the material to be experimentally identified. If this criterion is applied to a linear stress path characterized by $\alpha = \sigma_2/\sigma_1$ for a material of the constitutive equation $\sigma_e = K\epsilon_e^n$, the following equation is obtained:

$$P = \frac{K}{(1-\alpha_1+\alpha_1^2)^{1/2}} \int_0^{\epsilon_{en}} \epsilon_e^n \, d\epsilon_e + \frac{K}{(1-\alpha_2+\alpha_2^2)^{1/2}} \int_{\epsilon_{es}}^{\epsilon_{ef}} \epsilon_e^n \, d\epsilon_e \quad (2)$$

where ϵ_{en} is the equivalent strain at necking, α_1 and α_2 are associated to the two branches of the strain path before and after necking, n is the constant strain hardening exponent, and K is a constant.

As the second strain path is plane strain ($\alpha_2 = 0.5$) the equivalent strain at fracture is given by

$$\epsilon_{ef} = \left\{ \frac{3^{1/2}P}{2K}(n+1) - \epsilon_{es}^{(n+1)} \times \left[\frac{3^{1/2}}{2(1-\alpha+\alpha^2)^{1/2}} - 1 \right] \right\}^{1/(n+1)} \quad (3)$$

This calculation requires knowledge of the parameter ϵ_{es}, i.e. the FLDN.

For a first strain path in plane strain, the fracture strain is simply given by

$$\epsilon_{ef}^0 = \left[\frac{3^{1/2}P}{2K}(n+1) \right]^{1/(n+1)} \quad (4)$$

which is the best way to identify the parameter P.

Fig. 3 shows a plot of the calculated FLDF associated with a given FLDN, for a value of $P/K = 0.7$ and for two cases of constitutive behaviour: (a) with the constant strain hardening exponent $n = 0.2$, and (b) $n = 0.2$ in the range $\rho = \epsilon_2/\epsilon_1 \leqslant 0$, n varies linearly with ρ from 0.2 to 0.4 in the stretching region: $\rho > 0$. The shape of the FLDF obtained is roughly linear with a different shape according to the hardening behaviour.

2.2. Oyane criterion

The crition is given by

$$\int_0^{\epsilon_{ef}} \left(1 + \frac{1}{d}\frac{\sigma_m}{\sigma_e}\right) d\epsilon_e = \int_{\epsilon_{vo}}^{\epsilon_{vf}} \frac{\gamma f^2}{d} \, d\epsilon_v = b \quad (5)$$

where $\gamma = \rho_v/\rho_{vo}$ is the relative density of the material during straining; $f = 1/3 \times \{1 + [\gamma/(1-\gamma)]^{1/2}\}$; $\epsilon_v = \ln(v/v_0) = -\ln \gamma$ is the volume strain; d is a constant of the material; b is a constant related to volume damage as given by the second integral of the criterion; σ_m, σ_e and ϵ_e are the mean stress, the equivalent stress and strain, respectively.

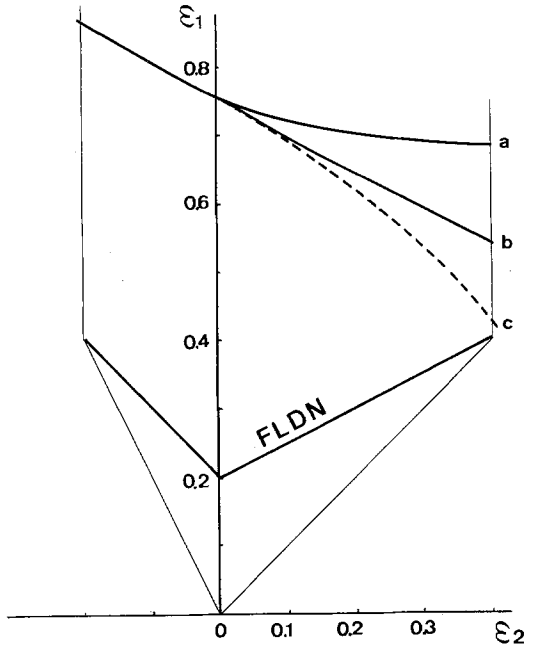

Figure 3 Theoretical FLDF obtained from: (a) the Latham and Cockroft criterion with strain hardening depending on the strain path, (b) the Latham and Cockroft criterion with constant strain hardening, and (c) the Oyane criterion.

Taking account of the two strain paths and introducing the plane strain value for the second one, the fracture strain is given by

$$\epsilon_{ef} = \frac{3^{1/2}d}{3^{1/2}d+1} \times \left\{ b - \frac{\epsilon_{es}}{3^{1/2}d} \left[\frac{1-\alpha}{3^{1/2}(1-\alpha+\alpha^2)^{1/2}} - 1 \right] \right\} \quad (6)$$

In order to compare the shape of the FLDF obtained by this criterion with the one of Latham and Cockroft (L & C), the parameters b and d have been identified on the level of the FLDF in Fig. 3 in the case of uniaxial deformation and plane strain. The obtained FLDF has then been plotted on the same figure and it can be seen that there is a lower FLDF with the Oyane criterion in comparison to the L & C criterion in equibiaxial stretching.

The fact that this criterion involved two parameters (b and d) instead of one (P) in the L & C criterion allows adjustment of the level on the

FLDF and also the slope. Furthermore, one of the parameters, b, can be related to internal damage.

3. Microscopic criteria

Microscopic criteria can be used to develop models to describe the coalescence process between voids. Some take account of the stress distribution between voids [12] but can only be applied in plane strain deformation, while others suppose brittle fracture between voids [13], but identification of the parameters generally gives higher values than expected.

The approach presented here is to start with the two main types of internal damage [5]: (i) damage by decohesion of the particle matrix interface, and (ii) damage by failure of the particle.

The void growth equation has been established [5]:

$$\epsilon_i^v = B_i \epsilon_1^\infty \tag{7}$$

where ϵ_i^v is the radial deformation of the void, $d\epsilon_i^v = dr_i/r_i$, and ϵ_1^∞ is the applied major principal strain. B_i is a strain concentration factor given by – in the case of damage of decohesion:

$$B_i = c\,\epsilon_i^\infty/\epsilon_1^\infty + 0.64(1+\rho) \tag{8}$$

where c is a constant parameter, and $\rho = \epsilon_2/\epsilon_1$. In the case of damage by failure the strain concentration factor is given by:

$$B_1 = \zeta = \text{cst}, B_2 = B_3 = 0$$

if the 1 direction coincides with the rolling direction or the direction of extension of the cracks opened by failure of the particle.

3.1. Damage by decohesion

The fracture surface resulting from this damage is of the ductile type and exhibits large cupules. Fig. 4 shows a zone of the fracture surface where the coalescence between two cavities is clear. Observation of the voids in a zone neighbouring the fracture surface shows the coalescence process at strains lower than the fracture strain because of the severe strain gradient near fracture. Generally, coalescence can be observed in the direction of the major principal strain (Fig. 5) [14]. Obviously ultimate fracture occurs in a plane normal to the principal strain by rapid coalescence of the big voids obtained in the primary coalescence along the major strain direction.

According to the observations that show an important growth of the cavities to the point where their proximity is dangerous, a geometrical model is used. The coalescence is assumed to occur when the spacing between cavities reaches a critical value compared to the dimension of the cavity itself (Fig. 6):

$$L_i = \alpha r_i \tag{9}$$

where L_i is the spacing between cavities and r_i the radial dimension in the i direction.

A perfectly ductile coalescence corresponds to $\alpha = 2$. The cavities are supposed to be distributed

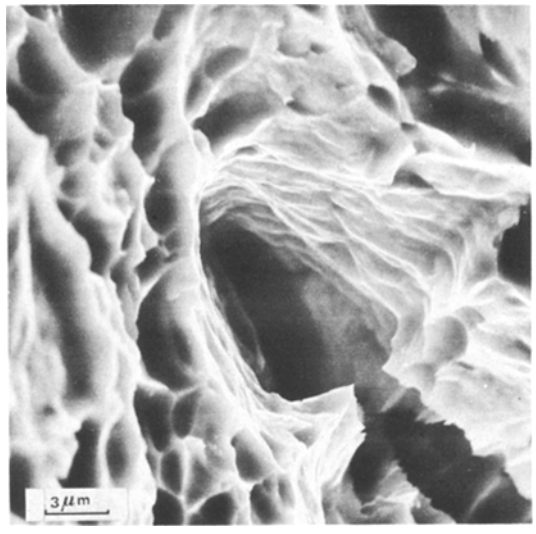

Figure 4 SEM observation of the coalescence process on the fracture of an AK steel.

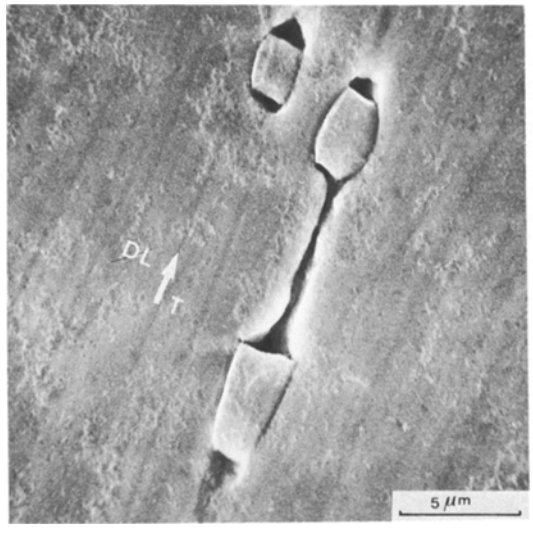

Figure 5 Coalescence between two cavities along the tensile axis, T, in a tough-pit copper deformed under uniaxial tension. (DL is the rolling direction.)

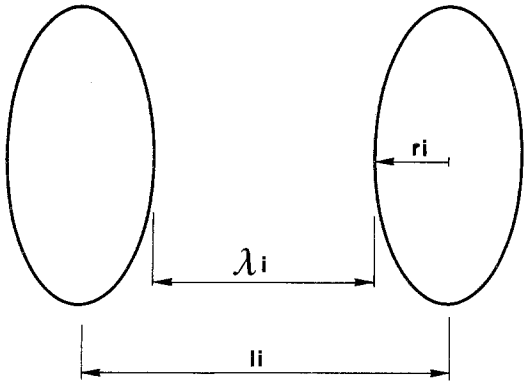

Figure 6 Parameters for the analysis of coalescence in the case of damage by decohesion.

at the edges of an octahedral shape (Fig. 7). The initial size and spacing of the voids is determined by the mean initial volume of the voids and mean spacing between first neighbours determined by scanning electron microscopic (SEM) observations.

It is possible, from an initial given distribution of spherical voids of the same shape to predict the evolution of the representative cube of Fig. 7 as the dimensions change according to the deformation applied and the void growth model.

The criterion is always verified first in the 1 direction of major principal strain in agreement with the observations previously reported in Fig. 5 where the value of the parameter α is about 4. When the criterion is verified, it means that the proximity of the cavities is sufficient to initiate a continuous process of coalescence, since when two voids coalesce in the 1 direction, overlap of voids in the 2 direction becomes more important, and as a consequence the area bearing the load is weakened and fails leading to macroscopic fracture. The overlap of voids in the 2 direction, without coalescence in the 1 direction, is obtained for a value of α equal to 4 for the regular network of cavities used.

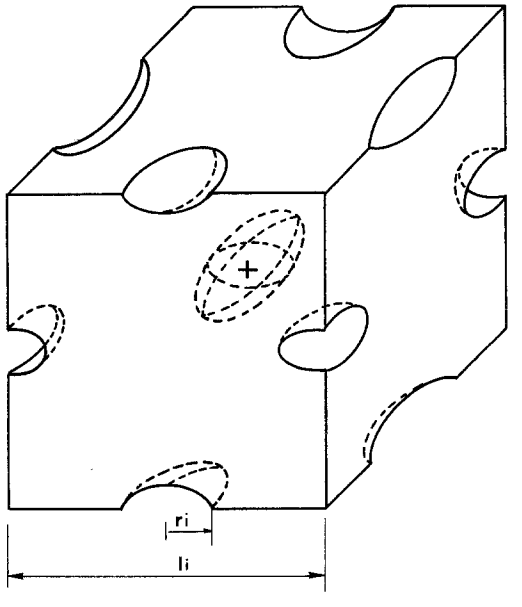

Figure 7 Representative elementary cube of the material.

The evolution of the spacing and size of the cavities is given by

$$l_1 = l_0 \exp(\epsilon_1) \tag{10}$$

$$r_1 = r_0 \exp(B_1\ \epsilon_1) \tag{11}$$

$$\text{where } B_1 = (c + 0.64) + 0.64\ \rho$$

Then at necking:

$$l_{1n} = l_0 \exp(\epsilon_{1s}) \tag{12}$$

$$r_{1n} = r_0 \exp(B_1\ \epsilon_{1n}) \tag{13}$$

Let the difference of the levels between the FLDN and FLDF be x:

$$x = \Delta\epsilon_1 = \epsilon_{1f} - \epsilon_{1n} \tag{14}$$

Between necking and fracture the evolution of the geometrical parameters is:

$$l_1 = l_{1n} \exp(x) \tag{15}$$

$$r_1 = r_{1n} \exp(B_1^0\ x) \tag{16}$$

Introducing the coalescence criterion, it becomes:

$$x = \frac{1}{(c-0.36)} \ln\left(\frac{l_0}{\alpha r_0}\right) - \left[1 + \frac{0.64}{(0.36-c)}\ \rho\right] \epsilon_{1n} \tag{17}$$

Using the assumption of plane strain deformation between necking and fracture, the following relation between the strains can be used:

$$\epsilon_{2f} = \epsilon_{2n} = \rho\ \epsilon_{1n} \tag{18}$$

which finally gives

$$\epsilon_{1f} = \frac{1}{(c-0.36)} \ln\left(\frac{l_0}{\alpha r_0}\right) - \frac{0.64}{(c-0.36)}\ \epsilon_{2f} \tag{19}$$

This equation is the analytical equation of the FLDF.

For a constant value of the parameter c, the FLDF is a straight line of slope, p_0, given by:

$$P_0 = -0.64/(c-0.36) \tag{20}$$

Such a line is experimentally observed and the experimental slope is of the order of:

$$-P_0 \in [0.5, 1.5] \tag{21}$$

which imposes for the parameter c:

$$c \in [0.8, 1.6] \tag{22}$$

This parameter c, taken from the Rice and Tracey [15] model of cavity growth is calculated to be 1.66 by the authors in the case of a spherical cavity in a non-hardening matrix. Another proposal [16] gives, for a two-dimensional problem, the change of the c parameter with the shape of the void:

$$c = 1 + (R_2/R_1) \tag{23}$$

which gives for a sphere: $c = 2$ and an infinite cylinder $c = 1$. The values obtained in this analysis are reasonable if they are taken as mean values of the parameter c over all the changes in shape of the voids involved by the total deformation process. A value of $c = 1.0$ can be used as a first approximation.

The slope of the FLDF depends on the c parameter, which is influenced by the shape of the voids and the hardening of the matrix. The level of the FLDF also depends on the parameter c and principally on the initial damage and the criterion parameter α. In the case of a plane strain deformation for the first stage of the strain path, the level of the FLDF is given by

$$\epsilon_{1f}^0 = \frac{1}{(c-0.36)} \ln\left(\frac{l_0}{\alpha r_0}\right) = 1.56 \ln (l_0/\alpha r_0) \tag{24}$$

using the assumption $c = 1.0$.

If we want to identify the value of the parameter α, it is necessary to know the level of the FLDF and the amount of initial damage. For an AK steel the level of the FLDF in plane stress is about

$$\epsilon_{1f}^0 = 1.5 \tag{25}$$

The initial damage can be determined by SEM observations, and the mean volume fraction of the voids is estimated to be

$$C_{vo} \in [5\ 10^{-4},\ 2\ 10^{-3}] \tag{26}$$

But fracture will occur in a region of most important concentration of voids. Fig. 8 [17] shows the probability of obtaining a volume fraction $C'_{vo} = x\, C_{vo}$ in a material containing a mean

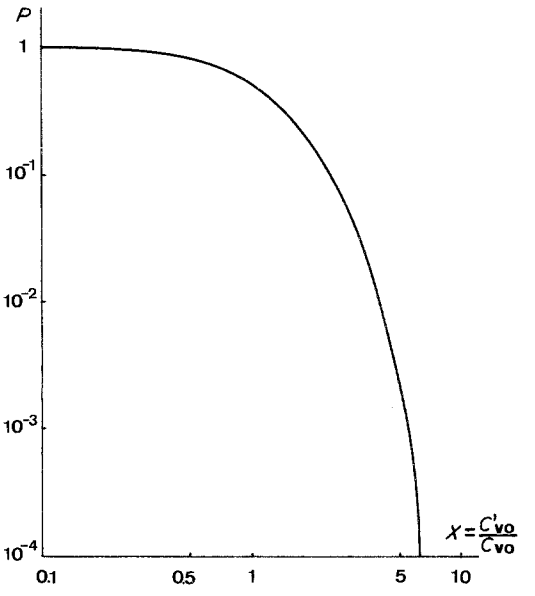

Figure 8 Probability of finding a volume fraction greater or equal to $x\, C_{vo}$ in a material of mean volume fraction C_{vo}.

volume fraction C_{vo}. According to previous work [18, 19], the probability in the necking or fracture zone, is estimated to be 10^{-4}, which leads to a volume fraction of voids seven times greater than the mean value:

$$C'_{vo} \in [3.5\ 10^{-3},\ 1.4\ 10^{-2}] \tag{27}$$

From the shape of the representative cube of the material in the fracture zone it becomes

$$\alpha = 0.72\, (C'_{vo})^{-1/3} \tag{28}$$

which gives

$$\alpha \in [4,\ 6.5] \tag{29}$$

Another way to look at this value is to express the criterion as a function of the dimension of the matrix between voids, λ_i (Fig. 6) and the diameter of the cavities d_i:

$$\lambda_i = \beta d_i = (\alpha - 2)\, r_i \tag{30}$$

which gives

$$\beta \in [1,\ 2.25] \tag{31}$$

This result is in agreement with observations [20, 21] where it is reported that coalescence occurs when the dimension of the matrix between voids is equal to once or twice the diameter. It should be noticed that a value of $\alpha = 4$ ($\beta = 1$), which is the condition of overlap between voids in the 2 direction, needs a volume fraction of

voids 20 times greater in the fracture zone to agree with experiment. Such concentration of cavities is obtained for an unrealisticly low value of probability (less than 10^{-20}). A similar criterion by Brown and Embury [22] consists in writing that the dimension of the matrix between the cavities in the 2 direction (direction of fracture) is equal to the larger dimension of the void (i.e. in the 1 direction): $\lambda_2 = d_1$. A comparison with our approach requires a change in the value of the α parameter with the strain path in a range: $\alpha \in [3, 5]$ to fit the Brown and Embury criterion. A calculation made with this last criterion [16], assuming only one linear strain path up to fracture, gives results in agreement with experiment but do not provide evidence, in an analytical equation of the FLDF, for the roles of the different parameters as they appear in this analysis.

The model proposed in this work is compatible with other models used and has the advantage of predicting the linear shape of the FLDF and to give its analytical equation where the following values of the parameters can be proposed:

$$c = 1.0$$
$$\alpha = 5$$
$$l_0/r_0 = 1.3\, C_{vo}^{-1/3}$$

where C_{vo} is the mean volume fraction of voids in the initial state or just after nucleation.

It should be noticed that the fracture strain, ϵ_{3f}, is not constant at fracture as proposed by a macroscopic fracture criterion [23]. In this model:

$$-\epsilon_{3f} = \frac{1}{(c-0.36)} \ln\left(\frac{l_0}{\alpha r_0}\right) + \left[1 + \frac{0.64}{(0.36-c)}\right]\epsilon_{2f} \tag{32}$$

which shows that the fracture strain is generally not constant for all the FLDF except when $c = 1.0$, the slope then being equal to -1.

3.2. Damage by failure

In contrast to damage by decohesion, the crack opened by failure of the particle always remains relatively small. It is therefore impossible to obtain for this type of damage the same coalescence process as in the case of decohesion. SEM observations near the fracture zone do not show any large cavity [24–26]. The coalescence mechanism cannot be observed, and so must be abrupt and occur when the cavities are relatively small and far from each other.

In this work it is proposed, after the work of McClintock [27], that coalescence proceeds by shear band instability between cavities. From the work of McClintock, the moment at which the instability occurs is given by [27]

$$\gamma_e = \frac{\partial \ln \sigma_e}{\partial \epsilon_e} = 3^{1/2} \frac{h_3 (h_1^2 + h_2^2)^{1/2}}{l_2 l_3} \tag{33}$$

where h_i and l_i are the size of the cavities and their spacing in the i direction, respectively.

In this model, fracture occurs when the rate of hardening decreases to a critical value controlled by the geometry of the distribution of the damage. The distribution of the cavities is assumed to be the same as that in the case of decohesion and the constitutive equation of the material is taken as

$$\sigma_e = K \epsilon_e^n \tag{34}$$

which leads to

$$\gamma_e = n/\epsilon_e \tag{35}$$

As in the case of the calculation of the FLDF according to the Latham and Cockroft criterion (Fig. 3), the hardening behaviour of the matrix will be treated in two cases: (i) with constant hardening exponent: $n = 0.2$, and (ii) with constant hardening exponent: $n = 0.2$ in the range $\rho = \epsilon_2/\epsilon_1 \leqslant 0$, linear variation of the strain hardening from 0.2 to 0.4 when ρ changes from 0 to 1.

It is further assumed that the dislocation structure developed during the first stage of the strain path is sufficiently stable to impose the same work hardening exponent during the second stage in plane strain.

The damage growth equation can be written:

$$h_1 = h_0 \exp(\zeta \epsilon_1) = h_0 \exp(\zeta \epsilon_{1n} + x) \tag{36}$$
$$h_2 = h_{0_2} \tag{37}$$
$$h_3 = h_{0_3} \tag{38}$$

where $x = \Delta\epsilon_1 = \epsilon_{1f}/ - \epsilon_{1s}$.

After some transformations, the following equation giving x is obtained:

$$\frac{2 \times 2^{1/2} h_{0_2}}{l_0^2 n} \frac{\{h_0^2 \exp[2\zeta(\epsilon_{1n} + x)] + h_{0_2}^2\}^{1/2} [(1 + \rho + \rho^2)^{1/2} \epsilon_{1n} + x]}{\exp[-(\epsilon_{1n} + x)]} = 1 \tag{39}$$

To solve this equation it is necessary to know the level of the FLDN, ϵ_{1n}, the initial configuration

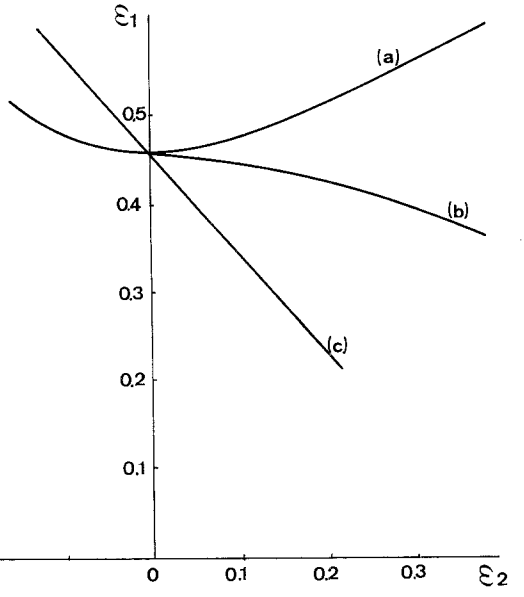

Figure 9 Theoretical FLDF obtained in the case of: (a) damage by failure with strain hardening depending on the strain path, (b) damage by failure with constant strain hardening, and (c) damage by decohesion.

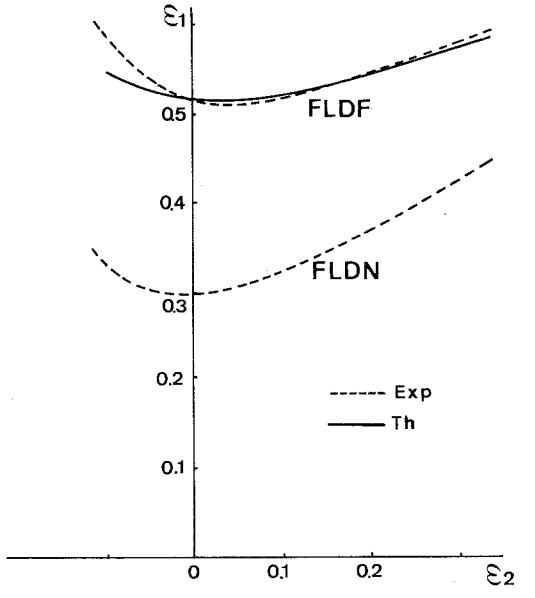

Figure 10 Comparison between calculated and experimental FLDF for a 3003 aluminium alloy presenting damage by failure of the precipitates.

of the cavities, h_{0i} and l_0, and the void growth parameter, ζ. Identification of ζ by relative density changes gives $\zeta \sim 4$.

Only in plane strain, the FLDF does not depend on the FLDN, as in this case ϵ_{1f} is given by

$$\frac{2 \times 2^{1/2} h_{0_3}}{l_0^2 n} \frac{(h_0^2 \exp(2\zeta \epsilon_{1f}) + h_{0_2}^2)^{1/2}}{\exp(-\epsilon_{1f})} \epsilon_{1f} = 1 \quad (40)$$

Fig. 9 shows a plot of the FLDF obtained, for the same level of plane strain, in the case of decohesion and in the case of damage by failure, both with hardening behaviour. It can be seen that the shape is curved in the case of damage by failure and that the slope in the stretching region ($\rho \geqslant 0$) can be positive.

Fig. 10 shows a plot of the calculated and the experimental FLDF of a 3003 aluminium alloy presenting damage by failure of the precipitates [5]. The following parameters have been derived from SEM observations: $h_{0_1} = 0.01$, $h_{0_2} = 3$, $h_{0_3} = 2, \zeta = 4, l_0 = 10$ (length in μm), and hardening behaviour depending on the strain path. The agreement between experimental and calculated FLDF is quite good and this shape of the FLDF is related to this type of damage, i.e. by failure of the particle.

4. Conclusions and discussion

This study shows that the type of damage controls the shape of the FLDF:

1. A linear straight line is associated with damage by decohesion.

2. A curved shape is associated with damage by failure.

The level of the FLDF is, in both cases, very dependent on the amount of initial damage.

The calculation proposed gives an analytical equation of the FLDF in the case of damage by decohesion which does not depend either on the shape and level of the FLDN or on the rheology of the material. In contrast, in the case of damage by failure, the FLDF can only be numerically determined and depends on the parameters mentioned above.

It should be noted that in most industrial materials, on the fracture surface many very small cupules can be observed between large ones. This phenomenon is not taken in account in this study.

According to the shape of the FLDF obtained, it seems that the Latham and Cockroft, and Oyane criteria are related to the case of damage by decohesion. A comparison can be carried out between these calculations. In fact, the L & C criterion involved only one parameter P that can be identified by the level of the FLDF in plane strain. A comparison with the model proposed gives

$$\epsilon_{1f}^{0} = \tfrac{3}{4}(n+1)\left(\frac{P}{K}\right)^{1/(n+1)} = \frac{1}{(c-0.36)}\ln\left(\frac{l_0}{\alpha r_0}\right) \quad (41)$$

The parameter P appears to depend on the matrix rheology, the amount of initial damage and the two parameters of the model, c and α.

It is more difficult to show such relation with the Oyane criterion, but it is nevertheless remarkable to notice that the Oyane criterion involves two parameters to identify b and d and that the model developed also involves two parameters, c and α. The advantage of the model proposed in this work is that the values of the parameters depending on the material can be determined by metallurgical observations and not only be identified afterwards by experiment. In this way a physical model can be more efficient than a mechanical one in order to predict the behaviour of a given material.

Acknowledgements

The author expresses his thanks to Professor B. Baudelet for discussing this work and to Dr J. H. Schmitt for fruitful discussions on the case of damage by failure.

References

1. M. GRUMBACH and G. SANZ, Meeting of the International Deep Drawing Research Group, Amsterdam, October 1972.
2. G. LEROY and J. D. EMBURY, "Internal Report no. 115" (McMaster University, Canada, 1977).
3. J. LEMAITRE and J. L. CHABOCHE, *J. Mech. Appl.* **3** (1978) 317.
4. C. M. KATCHANOV, *Izv. Akad. Nank. SSR otd. Tekh. Nank.* **8** (1958) 26.
5. J. H. SCHMITT and J. M. JALINIER, *Acta Metall.* **30** (1982) 1789.
6. M. G. COCKROFT and D. J. LATHAM, *J. Inst. Met.* **96** (1968) 33.
7. M. OYANE, *Bull. JSME* **15** (1972) 1507.
8. M. OYANE, T. SATO, K. OKIMOTO and S. SHIMA, *J. Mech. Work. Tech.* **4** (1980) 65.
9. D. M. NURIS, J. E. E. REAUGH, M. MORAN and D. F. QUINONES, *J. Eng. Mater. Tech.* **100** (1978) 279.
10. J. W. HANCOCK and A. C. MACKENZIE, *J. Mech. Phys. Solids* **24** (1976) 147.
11. P. W. BRIDGMAN, "Large plastic flow and fracture" (McGraw Hill, New York, 1952).
12. P. F. THOMASON, *J. Inst. Met.* **96** (1968) 360.
13. A. K. GOSH, *Met. Trans.* **7A** (1976) 523.
14. J. H. SCHMITT, J. M. JALINIER and B. BAUDELET, *J. Mater. Sci.* **16** (1981) 95.
15. J. R. RICE and D. M. TRACEY, *J. Mech. Phys. Solids* **17** (1969) 201.
16. G. LEROY, J. D. EMBURY, G. EDWARD and M. F. ASHBY, *Acta Metall.* **8** (1981) 1509.
17. A. S. ARGON, J. IM and R. SAFOGLU, *Met. Trans.* **6A** (1975) 825.
18. J. M. JALINIER and J. H. SCHMITT, *Acta Metall.* **30** (1982) 1799.
19. J. M. JALINIER, J. H. SCHMITT, R. ARGEMI, J. L. SALSMANN and B. BAUDELET, *Mem. Sci. Rev. Met.* **3** (1980) 313.
20. I. A. FRENCH and P. F. WEINRICH, *Met. Trans.* **6A** (1975) 785.
21. J. GURLAND, *Acta Metall.* **20** (1972) 735.
22. L. M. BROWN and J. D. EMBURY, in Proceedings of the 3nd International Conference on the Strength of Metals and Alloys, Cambridge, England, 1973, p. 164.
23. Z. MARCINIAK, "Lectures at McMaster University" (McMaster University, Hamilton, Canada, 1973).
24. S. FLOREN and M. W. HAYDEN, *Met. Sci. J.* **4** (1970) 77.
25. *Idem, Scripta Metall.* **4** (1970) 87.
26. A. MELANDER, "Internal Report TRITA-MAC-0142" (Royal Institute of Technology, Stockholm, Sweden, 1978).
27. F. A. McCLINTOCK, "Ductility" (ASM, Metals Park, Ohio, 1968) p. 255.

Received 20 September
and accepted 23 November 1982